03

Isotopically Modified Silicon Carbide: A Semiconductor Platform for Quantum Technologies

© E.N. Mokhov, S.S. Nagalyuk, O.P. Kazarova, S.I. Dorojkin, V.A. Soltamov

Ioffe Institute,
St. Petersburg, Russia

E-mail: Mokhov@mail.ioffe.ru

Received November 20, 2024
Revised November 25, 2024
Accepted November 26, 2024

This paper discusses the trends and approaches in developing the material base for quantum technologies using silicon carbide enhanced through isotope engineering. A comprehensive review of international research projects focused on the study and development of isotopically modified silicon carbide as a cutting-edge platform for quantum technologies is presented. The paper includes results from the characterization of isotopically modified 2″ (2 inch) ^{28}SiC produced at the Ioffe Institute, using secondary ion mass spectrometry, optical spectroscopy, and microwave spectroscopy. The study identifies two families of optically active spin centers in irradiated isotopically modified crystals: triplet centers ($S = 1$), including divacancies (V_{Si}-V_C) and nitrogen-vacancy (NV) defects, and quadruplet centers ($S = 3/2$), associated with negatively charged silicon vacancies (V_{Si}^-). These spin centers are widely utilized in the development of quantum sensors, qubits, and other quantum information technologies. The findings open new possibilities for exploring the properties of optically active high-spin centers in isotopically pure silicon carbide matrices.

Keywords: Silicon Carbide, isotope engineering, Silicon vacancy, divacancy, NV- defect, microwave spectroscopy.

DOI: 10.61011/PSS.2025.01.60588.316

1. Introduction

Modern quantum technologies require the development of new materials with unique properties [1,2]. The creation of isotopically pure semiconductors, in particular, silicon carbide is one of the promising fields in this respect [3–5]. This material has several advantages, combining the semiconductor properties of silicon, strength, thermal conductivity and chemical resistance of diamond.

Of particular interest are optically active defects in SiC, which have a high-spin ground state. Defects such as divacancies, NV-centers, and silicon vacancy centers can be used for quantum information processing, quantum magnetometry, and thermometry, as well as biosensors with submicron spatial resolution [1–5].

It is necessary to control the isotopic composition of the material for the effective application of SiC in quantum technologies. Isotopically unmodified SiC contains 4.7% of ^{29}Si isotope with nonzero nuclear spin ($I = 1/2$), which may limit the coherence times of quantum states [3–5]. Isotopic enrichment can significantly reduce the content of ^{29}Si, replacing it with stable non-magnetic isotopes of silicon ^{28}Si ($I = 0$, 92.2%), ^{30}Si ($I = 0$, 3.1%), thereby increasing the spin coherence times of defects [3–6].

Work aimed at obtaining isotopically modified silicon carbide for quantum technologies is currently actively underway in many research institutes and groups and is supported in all major countries at the level of national development programs. As an example, it makes sense to analyze the development of this field in Europe and the USA. Fraunhofer IISB has been studying the SiC growth using the isotopes ^{28}Si and ^{12}C since 2023 to improve the characteristics of qubits and single-photon sources based on spin defects. SPINUS project [7] funded by the Horizon Europe program, develops experimental platforms based on spin qubits for quantum simulations and calculations, with the participation of 12 partners from different European countries. QRC-4-ESP project (Quantum Reservoir Computing for Efficient Signal Processing) [8] launched in 2024, aims to create quantum computing systems using superconducting qubits and defects in SiC. QRC-4-ESP includes 7 university centers and research organizations from various European countries, including Germany, Great Britain, Sweden, France, Finland, Hungary and Switzerland. SiCqurTech (Silicon Carbide Qubits towards a Fab-Ready Technology) project [9] develops the integration of spin centers in SiC into photonic chips for quantum communication networks, focusing on technologies ready for industrial production, which is justified due to the fact that two-inch technology is well mastered in the case of silicon carbide. The project involves institutions such as the Luxembourg Institute of Science and Technology (LIST), Friedrich-Alexander University and ETH Zürich from Switzerland. Active studies in the field of SiC-based quantum technologies are also conducted in the USA. Several scientific consortia have been established for this purpose. Established in 2020, Q-NEXT [10] brings together roughly 100 experts from three national laboratories, 10 universities and 14 technology companies. Quantum Science Center of Q-NEXT studies spin defects in SiC for quantum sensors, memory, and quantum communication. Oak Ridge National Laboratory

ORNL [11] studies defects in SiC, investigating the effect of isotopes on the properties of quantum centers. These studies are aimed at unlocking the potential of SiC as a platform for sustainable and scalable quantum systems, which is of key importance for the development of quantum technologies. It is worth emphasizing that the above examples include only large projects implemented within the framework of significant R&D programs or research centers created separately for these tasks.

Our group has been studying the growth of high-quality isotopically modified silicon carbide and its use in quantum technologies for a relatively long time. We have proposed some applications of isotopically modified silicon carbide for quantum technologies such as quantum magnetometers starting from 2015 [12], we also conducted pioneering studies of the coherent and spin properties of defects in such crystals [4,6], on the basis of which it is currently proposed to create quantum information systems. It is worth noting the recent results of the creation of negatively charged nitrogen vacancy defects in isotopically enriched 6*H*-^{28}SiC by irradiating the latter with high-energy particles (electrons, protons, neutrons) with subsequent annealing [13,14].

We demonstrate in this paper the possibility of growing high-purity silicon carbide with a diameter of 2″ (50.8 mm) by the sublimation method enriched in the nonmagnetic isotope ^{28}Si to 99.8%. We show the possibility of creating the main types of centers in such crystals, which are offered today for the development of quantum technologies. Namely, NV-centers and divacancies (P6/P7 or VV^{0}centers) with $S = 1$ [13–16], as well as negatively charged silicon vacancies (V_{Si}^-) with $S = 3/2$ [17,18]. The basic spin and optical properties of these defects are illustrated in Figure 1, *and* their spectroscopic characteristics are summarized in Table 1. As shown in Figure 1, these defects have an optically induced spin alignment that differs significantly from the Boltzmann distribution, which allows them to be used as optically addressable qubits [19,20], the basis for masers active in a wide temperature range, up to room temperature [21,22], and also, given the intense photoluminescence and high-tech nature of silicon carbide, to create sources of single photonic [17,20,23,24] and spin-photonic interfaces [1,3,25], which are the basis of quantum information technologies. The uniqueness of the results presented in this paper is to demonstrate the first successful steps towards scalable quantum technologies based on isotopically modified silicon carbide in an industrially developed two-inch technology. It is worth emphasizing that our results open up the opportunity for studying all three main color centers offered today for quantum technologies within a single crystal matrix with a controlled isotopic composition. This opens up prospects for a comparative analysis of their properties under identical conditions, which is especially important for optimizing the parameters of SiC-based quantum devices.

2. Experimental part

Crystals of silicon carbide 6*H*-^{28}SiC with a reduced content of the magnetic isotope ^{29}Si ($I = 1/2$) were grown by high-temperature physical vapor transport (PVT) [31] using a precursor enriched in the isotope ^{28}Si. 6*H*-SiC substrate with a natural content of silicon and carbon isotopes was used as a seed: ^{29}Si ($I = 1/2$, natural prevalence 4.7%), ^{28}Si ($I = 0$, 92.2%), ^{30}Si ($I = 0$, 3.1%), and ^{12}C ($I = 1/2$, 98.9%), ^{13}C ($I = 1/2$, 1.1%). A commercially available isotopically pure source of ^{28}Si in powder form produced by State Corporation „Rosatom“ was characterized by a purity level of 99.98% in terms of the content of the specified isotope. Thus, the content of stable isotopes in the precursor — the non-magnetic isotope ^{30}Si and the magnetic isotope ^{29}Si is reduced by more than 10 times. The concentrations of the main impurities in the grown sample and the isotopic composition of silicon in the grown samples were evaluated by secondary ion mass spectrometry (IMS 7f, CAMECA). The control measurement of the concentration of the isotope ^{28}Si was carried out by analyzing the intensity of the components of an ultrathin structure in the spectra of electron paramagnetic resonance (EPR) of V_{Si}^- centers. EPR spectra in both continuous and pulsed modes were recorded on commercial BrukerESP300 and E680 spectrometers in the frequency ranges of 9.4 GHz (X-band) and 94 GHz (W-band), respectively. Pulse spectra were obtained by recording the integral intensity of the electron spin echo (ESE) as a function of magnetic field sweep **B** using a sequence of Khan pulses $\pi/2$-τ-π-τ — ESE. The pulse duration $\pi/2$ is 44 ns, and $\tau = 280$ ns. The main part of the experiments was conducted at room temperature ($T = 300$ K) and with optical excitation by IR lasers ($\lambda = 785$; 808 and 980 nm). The ESE spectrum of divacancies was measured at a temperature of 50 K using a flow-through helium cryostat from Oxford Instruments to cool the sample. Microphotoluminescence experiments (μ-PL) were conducted using T64000 spectrometer (Horiba Jobin-Yvon, Lille, France) equipped with a confocal microscope and a silicon CCD matrix cooled to liquid nitrogen temperature. A laser $\lambda = 785$ nm was used to excite luminescence. The PL spectra were recorded using diffraction grating 600 grooves/mm. V_{Si}^- centers were created by irradiation of the grown sample by electrons with an energy of 2 MeV and a dose of $2 \cdot 10^{18}$cm^{-2}. Divacancies and NV$^-$ defects were created by the annealing of the irradiated sample at a temperature of 900°C for 2 h in an argon atmosphere [13,32].

3. Results and discussion

Figure 2 shows a photograph of a plate with a diameter of 2″ of single-crystal 6*H*-^{28}SiC. The same figure shows the results of the sample analysis by secondary ion mass spectrometry (SIMS) for the main uncontrolled impurities (nitrogen, oxygen, boron, aluminum) and isotopic composition. It can be seen from the SIMS data that the upper limit of the nitrogen concentration is $1.5 \cdot 10^{17}$cm^{-3}, and the concentration of *p*-type compensating impurities (B, Al) is an order of magnitude lower.

Thus, the grown sample contains a concentration of nitrogen admixture uncompensated by acceptors of the

Table 1. Designations of optically active V_{Si}^- centers with spin $S = 3/2$, NV^- centers and divacancies with spin $S = 1$ in 6*H*-SiC. The corresponding phononless lines in the PL spectra are given in nm, the values of the splits in the zero magnetic field (D for $S = 1$ and $2D$ for $S = 3/2$) taking into account the sign of the fine structure constant D, given in MHz

	V_{Si}^- [17,18,26]			NV^- [13,27]			VV^0 [28,29,30]		
ZPL	V_1	V_2	V_3	NV_{k1k2}	NV_{k2k1}	NV_{hh}	VV_{k1k2}	VV_{k2k1}	VV_{hh}
E, nm	865	887	906	1155	1227	1183	1139	1093	1135
ZFS, MHz	−27	+128	−27	+1355	+1278	+1328	+1300	+1342	+1334

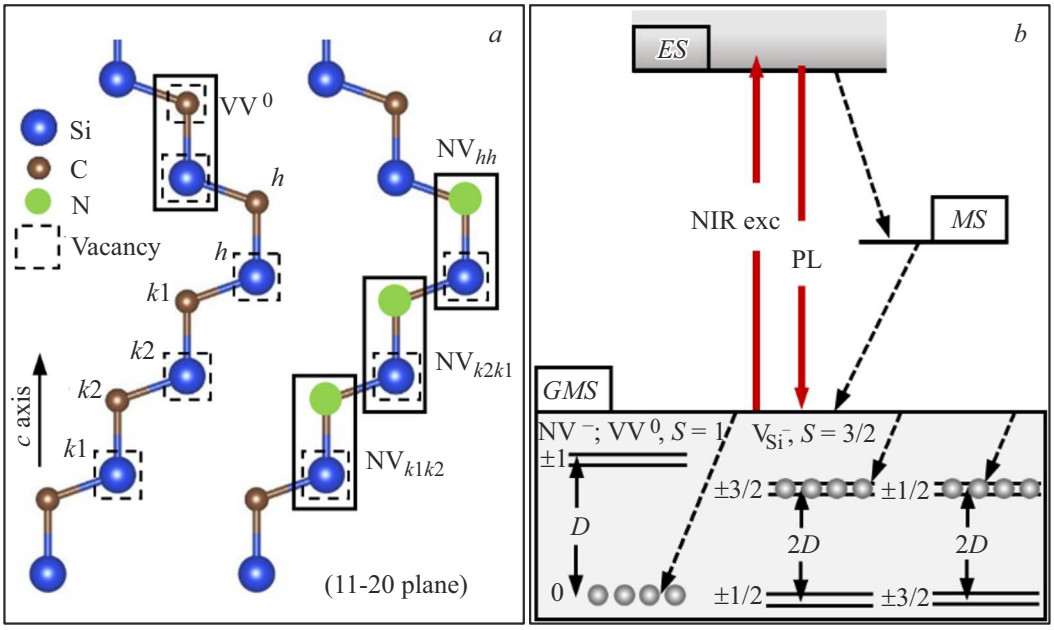

Figure 1. (*a*) View of 6*H*-SiC lattice in the plane $(11\bar{2}0)$. Silicon, carbon, and nitrogen atoms are shown in blue, brown, and green, respectively. The hexagonal (h) and quasi-cubic ($k1$, $k2$) unequal positions are indicated respectively. Vacancies of silicon and carbon are indicated by dotted lines, paired defects of NV and divacancies are shown by rectangles. (*b*) Energy structure of levels in the optical pumping cycle of spin sublevels of triplet centers (NV^-, VV^0) and quadruplet centers (V_{Si}^-). The dotted arrows show spin-dependent recombination from the excited state (ES) to the ground state (GS) through the metastable state (MS) under the action of near-infrared optical excitation (NIRexc). Spin-dependent IR luminescence is designated as NIRPL. The separation of spin sublevels in the absence of a magnetic field is indicated by the fine structure parameter D. Two ground state occupation diagrams are provided for V_{Si}^- depending on the sign of the fine structure parameter that determines the order of the spin sublevels.

order $10^{17}\,cm^{-3}$. Isotopic analysis shows that the degree of enrichment of the grown SiC sample with the non-magnetic 28 silicon isotope is 99.799%, which is in good agreement with the specification of the precursor, and a slight deviation of 0.1% can be explained by autoloading silicon from 6*H*-SiC substrate used as a seed.

Irradiation of 6*H*-^{28}SiC sample by electrons leads to the creation of vacancy centers, of particular interest of which is the negatively charged silicon vacancy, characterized by spin and optical properties shown in Figure 1, *b* and the parameters specified in Table 1, namely, a set of phononless lines V1, V2, V3 in the photoluminescence spectrum, splitting of spin sublevels of the ground state $S = 3/2$ in a zero magnetic field, and optically induced alignment of spin sublevels. This set of characteristics is illustrated in Figure 3. Namely, the spectrum of low-temperature photoluminescence is shown in Figure 3, *a*. The three phononless lines V1, V2, V3 and their position in the spectrum clearly indicate the presence of silicon vacancies in the crystal in a negative charge state. Figure 3, *b* shows the EPR spectrum recorded in the X-band with the orientation of the magnetic field $\mathbf{B} \parallel \mathbf{c}$ and optical excitation of the sample by $\lambda = 808$ nm laser. This EPR spectrum unambiguously proves the presence of V_{Si}^- centers in the studied sample [17,19]. In this orientation of the magnetic field, the magnitudes of the magnetic field splits between the resonant components of the fine structure, indicated on the spectrum as $\Delta B(V2)$ and $\Delta B(V1,V3)$ are equal to 9.1 mT and 1.9 mT, respectively. Based on the fact that in this orientation $\Delta B = 4D/g\mu_B$, where g is a factor of 2.00, and

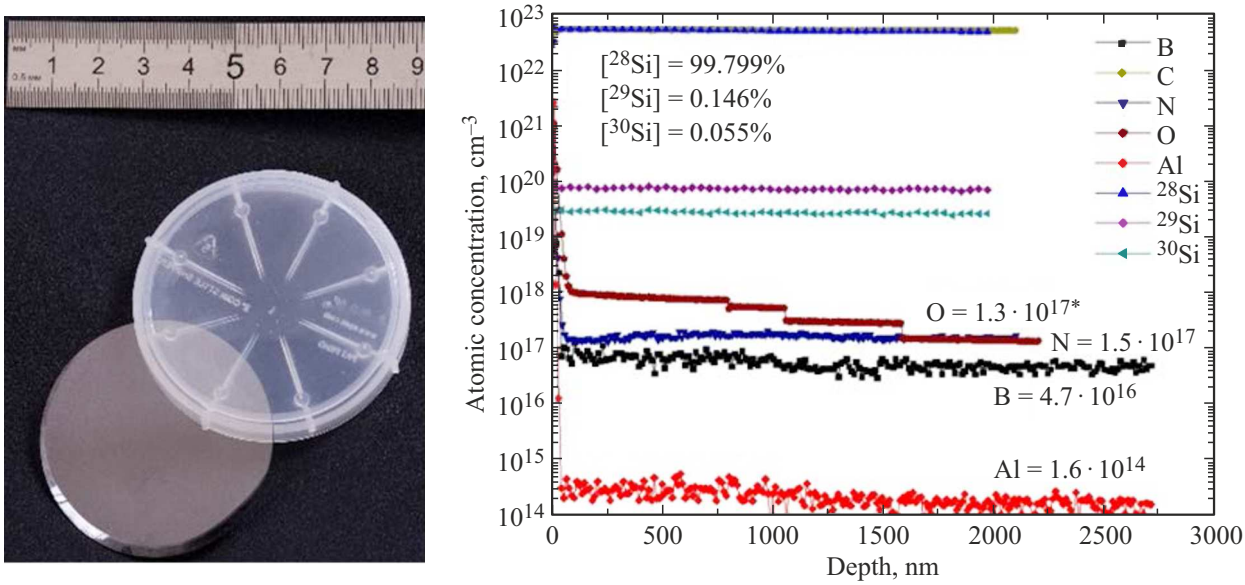

Figure 2. A photo of a polished plate of 2″ 6*H*-^{28}SiC is provided on the left. SIMS analysis data showing the concentrations of the main uncontrolled impurities are provided on the right: N, B, Al and the content of ^{28}Si, ^{29}Si, ^{30}Si isotopes.

μ_B is a Boron magneton, the ZFS value equal to $2D$ can be easily calculated as equal to 127.4 MHz for centers V2 and 26.6 MHz for centers V1/V3, which is in good agreement with Table 1. An important feature of the spectra is the phase inversion of EPR signals in each pair of fine-structure components, which indicates the creation of an optically induced alignment of spin sublevels, as schematically shown in Figure 1, *b* and in the insert of Figure 3, *b*.

After the presence of V_{Si}^- centers in isotopically pure SiC was unambiguously shown by a set of spectroscopic characteristics, we performed an independent additional assessment of the isotopic enrichment of silicon carbide with the non-magnetic silicon 28 isotope, taking into account that the intensity of the hyperfine interaction (HFI) satellites of the electron spin of V_{Si}^- centers with nuclear magnetic moments of the SiC lattice, observed in the EPR spectra (shown by arrows in the insert of Figure 3, *b*), are proportional to the concentration of the magnetic isotope ^{29}Si.

Indeed, the intensity of each fine structure line corresponds to the EPR transitions between the electron spin sublevels for which there is no HFI, that is, it corresponds to the interaction with the nuclear spins 28 and 30 of the silicon isotope, for which $I = 0$. The accompanying doublets of hyperfine lines with splitting 0.29 mT, occur as a result of HFI with one atom of ^{29}Si ($I = 1/2$) among the 12 nearest neighbors of the sublattice Si [33,34]. The intensity ratio between the total intensity of the two components of the HFI and the central line of the fine structure is 0.126. Taking into account that the intensity of the HFI line is determined by the probability of the presence of one ^{29}Si atom among the 12 nearest neighbors in the lattice Si (P_1), while the intensity of the center line is determined by the probability that all 12 Si atoms have $I = 0$ (P_0) it is possible to determine the concentration of ^{29}Si. Namely, the probability that a lattice site is occupied by an odd isotope is defined as $P_m = C_m^n X^m (1-X)^{n-m}$, where m is the number of nodes occupied by the isotope, n is the number of equivalent lattice sites considered in the calculations, and X is the isotope concentration ^{29}Si. Thus, $P_1 = 12 \cdot X \cdot (1-X)^{11}$ and $P_0 = (1-X)^{12}$. Using the intensity ratio of 0.126, we obtain $X = 0.0103$, which corresponds to ^{29}Si content of approximately 1% in the sample. Modeling of the shape of the EPR line, performed using Bruker BioSpin software, taking into account ^{29}Si content of 1%, is shown by red color in the insert in Figure 3, *b*. The good agreement between the experimental spectrum and the simulated spectrum confirms the correctness of our calculations. Thus, it follows from the EPR spectrum that the concentration of the magnetic ^{29}Si isotope is reduced by 4.7 times.

Table 2. Spectroscopic parameters of NV-centers used in calculating the positions of EPR lines according to the spin Hamiltonian (1)

Defect	g	D, MHz
NV_{k1k2}	2.0045	1358
NV_{hh}	2.0044	1331
NV_{k2k1}	2.0046	1282

Further, using pulsed EPR in the W-band (94 GHz), we studied irradiated 6*H*-^{28}SiC crystals annealed for two hours at a temperature of 900°C in an argon atmosphere to demonstrate the creation of isotopically pure samples of NV^- centers and divacancies. The EPR spectrum recorded in the electron spin echo mode with the orientation of the magnetic field $\mathbf{B} \parallel \mathbf{c}$ and with constant optical excitation by $\lambda = 964$ nm laser is shown in Figure 4. Three pairs of lines are observed in the spectrum, designated as NV_{hh},

NV_{k2k1} and NV_{k1k2}. The structure of the spectrum indicates splitting in a zero magnetic field between the spin sublevels of triplet defects. The spectrum can be described by a spin Hamiltonian of axial symmetry of the form (1), which includes a Zeeman term and a term reflecting the splitting of spin sublevels in a zero magnetic field, leading to the appearance of a fine structure in the EPR spectrum:

$$H = g\mu_B \mathbf{B} \cdot \mathbf{S} + D(S_z^2 - 2/3), \qquad (1)$$

where $\mathbf{S}$ is the electron spin operator, $\mathbf{B}$ is the constant magnetic field, D is the fine structure parameter corresponding to the ZFS value in Figure 1, *a*, S_z^2 is the spin projection operator of the triplet center. Calculation of the experimental spectrum using this Hamiltonian, performed in the EasySpin program with the parameters: $NV_{hh}g = 2.0044$, $D = 1331$ MHz;

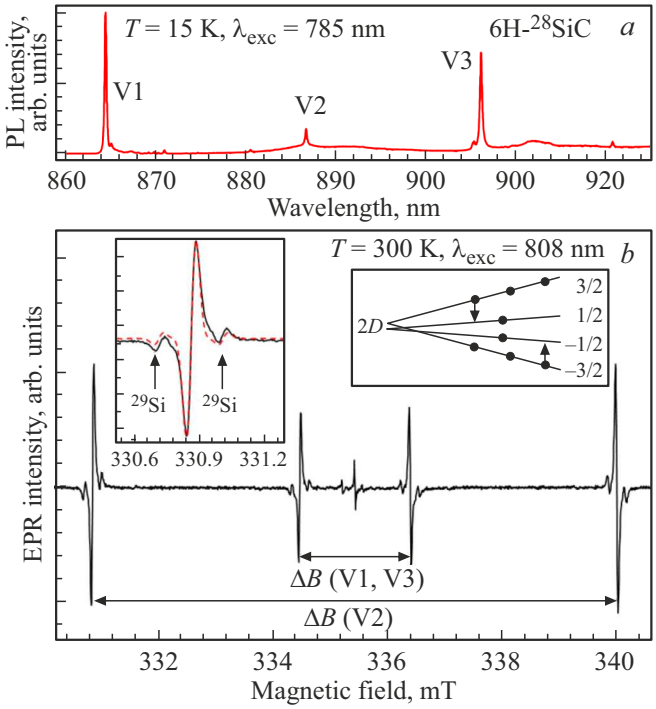

Figure 3. (*a*) Photoluminescence spectrum of an electron-irradiated 6*H*-^{28}SiC sample was detected with excitation by $\lambda = 785$ nm laser and temperature of $T = 15$ K. The set of phoneless lines of V_{Si}^- centers is indicated by the generally accepted abbreviation V1/V2/V3 [17,18]; the position of the lines corresponds to the data given in Table 1. (*b*) The EPR spectrum of 6*H*-^{28}SiC sample, recorded at room temperature and optical excitation of the sample with $\lambda = 808$ nm laser. The orientation of the permanent magnetic field is $\mathbf{B} \parallel \mathbf{c}$. The signals of the EPR centers V_{Si}^- are indicated by arrows. The insert on the right schematically shows the inverse occupation of spin sublevels under the action of optical pumping. The insert on the left shows the low-field component of V_{Si}^- centers in the magnified scale. The vertical arrows indicate the doublet of the HF component with splitting 0.29 mT, resulting from HFI with one atom ^{29}Si. The experimental spectrum is shown by a solid black line, and the modeled EPR line with a concentration of ^{29}Si 1% is shown by a dotted red line.

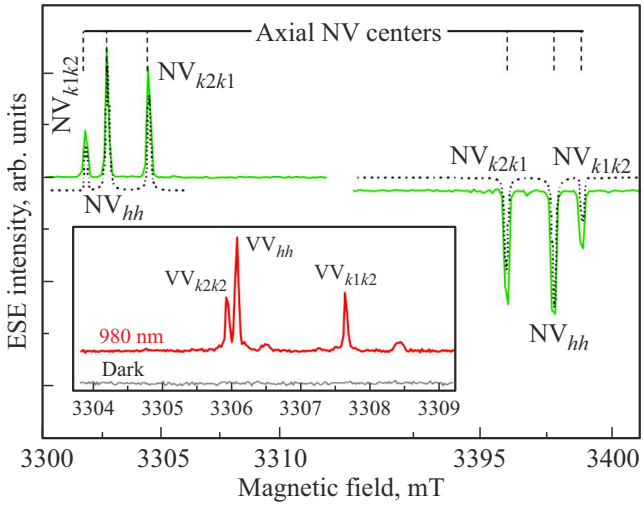

Figure 4. Pulse EPR spectrum of sample of 6*H*-^{28}SiC, irradiated with electrons and annealed at 900°C, recorded at $T = 300$ K and with excitation by $\lambda = 980$ nm laser. The orientation of the magnetic field is $\mathbf{B} \parallel \mathbf{c}$. The resonant magnetic fields corresponding to the allowed transitions between the spin sublevels of triplet centers are designated as NV_{hh}, NV_{k2k1} and NV_{k1k2}. The dotted line shows the calculated spectrum using (1) and the parameters of Table 2. The insert shows the spectra recorded at a temperature of $T = 50$ K with optical excitation by $\lambda = 980$ nm laser and without it (dark).

$NV_{k2k1}g = 2.0046$, $D = 1282$ MHz; $NV_{k1k2}g = 2.0045$, $D = 1358$ MHz, shown on Figure 4 by a dotted line. The triplet state and spectroscopic values correspond to NV^- centers of axial symmetry in 6*H*-SiC. The inversion of the signals of the high-field components of the fine structure inside each pair of triplet lines indicates the predominant occupation of the spin sublevel with the projection of spin $m_s = 0$ created by optical excitation. The insert of Figure 4 shows a fragment of the spin echo spectrum recorded at a temperature of $T = 50$ K. The lines in the spectrum, designated as VV_{hh}, VV_{k2k2} and VV_{k1k2}, correspond to another family of triplet centers, namely the divacancies (V_{Si}-V_C) in the neutral charge state [15,16].

4. Conclusion

This paper presents current trends in world scientific practice in the field of quantum technologies using industrial semiconductor material silicon carbide. We have demonstrated the possibility of obtaining of 2″ of a single-crystal 6*H*-^{28}SiC in Ioffe Institute of Physics and Technology using isotopically pure silicon obtained in ROSATOM as a precursor. Taking into account that the scientific and technological side of the study and production of various isotopes is traditionally considered one of the strongest sides of Russian science [33,34], the development of quantum technologies based on high-spin defects in isotopically pure SiC, in our opinion, is particularly promising. We also demonstrated the technology of creating spin centers, V_{Si}^-,

NV^- and VV^0, with the property of spin alignment under the action of optical pumping, in grown crystals. These results can be considered the basis and starting point for the development of quantum technologies based on isotopically modified silicon carbide.

Funding

This study was conducted under the state assignment FFUG-2024-0024 „Functional materials for microelectronics and photonics“.

Conflict of interest

The authors declare that they have no conflict of interest.

References

[1] D. Awschalom, R. Hanson, J. Wrachtrup, B.B. Zhou, Nat. Photonics **12**, 516–527 (2018).
[2] P.G. Baranov, H.J. von Bardeleben, F. Jelezko, J. Wrachtrup. Springer Series in Material Science. Springer, Heidelberg (2017).
[3] A. Bourassa, C.P. Anderson, K.C. Miao, et al. Nature Mater. **19**, 1319–1325 (2020).
[4] V.A. Soltamov, C. Kasper, A.V. Poshakinskiy, A.N. Anisimov, E.N. Mokhov, A. Sperlich, S.A. Tarasenko, P.G. Baranov, G.V. Astakhov, V. Dyakonov. Nat. Commun. **10**, 1678 (2019).
[5] I. Lekavicius, R.L. Myers-Ward, D.J. Pennachio, J.R. Hajzus, D.K. Gaskill, A.P. Purdy, A.L. Yeats, P.G. Brereton, E.R. Glaser, T.L. Reinecke, S.G. Carter, PRX Quantum **3**, 010343 (2022).
[6] V.A. Soltamov, B.V. Yavkin, A.N. Anisimov, H. Singh, A.P. Bundakova, G.V. Mamin, S.B. Orlinskii, E.N. Mokhov, D. Suter, P.G. Baranov. Phys. Rev. B **103**, 195201 (2021).
[7] URL: https://spinus-quantum.eu/ link to an electronic resource containing brief information about the SPINUS project (2024).
[8] https://www.qrc-4-esp.eu/ link to an electronic resource containing brief information about the project *qrc-4-esp*
[9] URL: https://quantera.eu/sicqurtech/ link to an electronic resource containing brief information about the *SiCqurTech* project
[10] URL: https://q-next.org/about/ link to an electronic resource containing brief information about the laboratory Q-NEXT
[11] URL: https://www.ornl.gov/quantum/ link to an electronic resource containing brief information about the ORNL laboratory
[12] D. Simin, V.A. Soltamov, A.V. Poshakinskiy, A.N. Anisimov, R.A. Babunts, D.O. Tolmachev, E.N. Mokhov, M. Trupke, S.A. Tarasenko, A. Sperlich, P.G. Baranov, V. Dyakonov, G.V. Astakhov. Phys. Rev. X **6**, 031014 (2016).
[13] F.F. Murzakhanov, Yu.A. Uspenskaya, E.N. Mokhov, O.P. Kazarova, V.V. Kozlovskii, V.A. Soltamov. Phys. SolidState **66**, 4, 537–541 (2024).
[14] F.F. Murzakhanov, M.A. Sadovnikova, G.V. Maminetal. JETP Lett. **119**, 593–598 (2024).
[15] V.S. Vainer, V.A. Il'in. Sov. Phys. Solid State **23**, 2126 (1981).
[16] R.A. Babunts, Yu.A. Uspenskaya, A.S. Gurin, A.P. Bundakova, G.V. Mamin, A.N. Anisimov, E.N. Mokhov, P.G. Baranov. JETPLett. **116**, 7, 485–492 (2022).
[17] P.G. Baranov, A.P. Bundakova, A.A. Soltamova, S.B. Orlinskii, I.V. Borovykh, R. Zondervan, R. Verberk, J. Schmidt. Phys. Rev. B **83**, 125203 (2011).
[18] V.A. Soltamov, D.O. Tolmachev, I.V. Il'in, G.V. Astakhov, V.V. Dyakonov, A.A. Soltamova, P.G. Baranov. Phys. Solid State **57**, 891–899 (2015).
[19] V.A. Soltamov, A.A. Soltamova, P.G. Baranov, I.I. Proskuryakov. Phys. Rev. Lett. **108**, 226402 (2012).
[20] D.J. Christle, P.V. Klimov, C.F. de las Casas, K. Szász, V. Ivády, V. Jokubavicius, J.U. Hassan, M. Syväjärvi, W.F. Koehl, T. Ohshima, N.T. Son, E. Janzén, Á. Gali, D.D. Awschalom. Phys. Rev. X **7**, 021046 (2017).
[21] H. Kraus, V.A. Soltamov, D. Riedel, S. Vath, F. Fuchs, A. Sperlich, P.G. Baranov, V. Dyakonov, G.V. Astakhov. Nature Phys. **10**, 157–162 (2014).
[22] A. Gottscholl, M. Wagenhöfer, V. Baianov, V. Dyakonov, A. Sperlich. arXiv:2312.08251 (2023).
[23] M. Widmann, S.-Y. Lee, T. Rendler, N.T. Son, H. Fedder, S. Paik, L.-P. Yang, N. Zhao, S. Yang, I. Booker, A. Denisenko, M. Jamali, S.A. Momenzadeh, I. Gerhardt, T. Ohshima, A. Gali, E. Janzén & J. Wrachtrup. Nature Mater. **14**, 164–168 (2015).
[24] Z. Mu, S.A. Zargaleh, H.J. von Bardeleben, J.E. Fröch, M. Nonahal, H. Cai, X. Yang, J. Yang, X. Li, I. Aharonovich, W. Gao. Nano Lett. **20**, 8, 6142–6147 (2020).
[25] C. Babin, R. Stöhr, N. Morioka, T. Linkewitz, T. Steidl, R. Wörnle, D. Liu, E. Hesselmeier, V. Vorobyov, A. Denisenko, M. Hentschel, C. Gobert, P. Berwian, G.V. Astakhov, W. Knolle, S. Majety, P. Saha, M. Radulaski, N.T. Son, J. Ul-Hassan, F. Kaiser, J. Wrachtrup. NatureMater. **21**, 67–73 (2022).
[26] T. Biktagirov, W. Gero Schmidt, U. Gerstmann, B. Yavkin, S. Orlinskii, P. Baranov, V. Dyakonov, V. Soltamov. Phys. Rev. B **98**, 195204 (2018).
[27] Kh. Khazen, H.J. von Bardeleben, S.A. Zargaleh, J.L. Cantin, Mu Zhao, W. Gao, T. Biktagirov, U. Gerstmann. Phys. Rev. B **100**, 205202 (2019).
[28] A.L. Falk, B.B. Buckley, G. Calusine, W.F. Koehl, V.V. Dobrovitski, A. Politi, C.A. Zorman, P.X.-L. Feng, D.D. Awschalom. Nat. Commun. **4**, 1819 (2013).
[29] P.G. Baranov, I.V. Il'in, E.N. Mokhov, M.V. Muzafarova, S.B. Orlinskii, J. Schmidt. JETP Lett. **82**, 441 (2005).
[30] J. Davidsson, V. Ivady, R. Armiento, T. Ohshima, N.T. Son, A. Gali, I.A. Abrikosov. Appl. Phys. Lett. **114**, 112107 (2019).
[31] Yu.A. Vodakov, E.N. Mokhov, M.G. Ramm, A.D. Roenkov. Krist. Tech. **14**, 729 (1979).
[32] W.E. Carlos, N.Y. Garces, E.R. Glaser, M.A. Fanton. Phys. Rev. B **74**, 235201 (2006).
[33] N.V. Abrosimov, D.G. Aref'ev, P. Becker, H. Bettin, A.D. Bulanov, M.F. Churbanov, S.V. Filimonov, V.A. Gavva, O.N. Godisov, A.V. Gusev, T.V. Kotereva, D. Nietzold, M. Peters, A.M. Potapov, H-J. Pohl, A. Pramann, H. Riemann, P-T. Scheel, R. Stosch, S. Wundrack, S. Zakel. Metrologia **54**, 599 (2017).
[34] Iz istorii FTI im. Ioffe. Vypusk 4. Boris Pavlovich Konstantinov (k 100-letiyu so dnya rozhdeniya). — SPb: Ioffe Physico-Technical Institute, 2010.

Translated by A.Akhtyamov